Mod Rheumatol (2002) 12:56–63

ORIGINAL ARTICLE

Hiroshi Orui · Masatoshi Takahara · Akira Ishikawa
Michiaki Takagi · Takashi Tsuchiya · Toshihiko Ogino

Radiological features of long bones in synovitis, acne, pustulosis, hyperostosis, osteitis syndrome and their correlation with pathological findings

Received: April 17, 2001 / Accepted: August 2, 2001

Abstract The purpose of this study was to demonstrate the radiological features of long bones in synovitis, acne, pustulosis, hyperostosis, osteitis (SAPHO) syndrome and to correlate these with the clinical findings. Eleven long bone lesions in seven cases of SAPHO syndrome were examined. The patients ranged in age from 6 to 63 years, with a mean of 47 years. In all seven cases, radiography, ^{99m}technetium bone scintigraphy, CT scan, and magnetic resonance imaging (MRI) were performed. In six of the cases, bone biopsy and bone culture were carried out for 7 long bones. Seven of the involved lesions were from the shaft of the femur, one each was from the neck and the shaft of the humerus, and one was from the proximal tibia. These lesions showed radiologically hyperostosis, osteolysis, and bone infarction-like lesion. Osteolysis was occasionally accompanied by sclerotic change. Hyperostosis usually showed diaphyseal involvement, presenting low signal intensity on T_1- and T_2-weighted MR images. Histologically, these findings corresponded to massive bone necrosis, new bone formation, fibrosis, or a mixture of these associated with mild inflammatory cell infiltration. Osteolysis involved dyaphysis, metaphysis, or epiphysis associated with arthritis, and presented low signal intensity on T_1-weighted images, nonhomogeneous signal intensity lower than fat on T_2-weighted images, and high signal intensity on fat suppression images. These findings corresponded to fibrosis, granulation, and inflammatory cell infiltration with lymphocyte aggregation. Bone infarction-like lesion was observed in the shaft or neck of the femur and the humerus and accompanied by calcification and cystic change. Bone cultures were negative in all cases in which bone biopsy was performed. Although hyperostosis is thought to be a characteristic bone lesion in SAPHO syndrome, the long bone lesion can occasionally show not only hyperostosis but also osteolytsis and bone infarction-like lesions.

Key words Bone infarction · Hyperostosis · Long bone · Magnetic resonance imaging (MRI) · Synovitis, acne, pustulosis, hyperostosis, osteitis (SAPHO) syndrome

Introduction

Since the first report of aseptic hyperostosis of the clavicle associated with palmoplantar pustulosis (PPP) by Sasaki in 1967,[1] similar cases of osteoarticular manifestation associated with dermatosis have been reported. The concept of synovitis, acne, pustulosis, hyperostosis, osteitis (SAPHO) syndrome was first presented by Chamot and colleagues in 1987,[2] for the disorders characterized by dermatologic and osseous manifestation such as severe acne, PPP, and axial or peripheral hyperostosis. Following their initial definitions, hyperostotic bone lesions such as sternoclavicular hyperostosis,[3] chronic sclerosing osteomyelitis (Garre)[4] and chronic recurrent multifocal osteomyelitis (CRMO),[5,6] and pustulotic arthro-osteitis[7] can be placed into this category. Furthermore, although controversial, an association with seronegative spondyloarthropathy or psoriatic arthritis[8,9] and the mechanism of these lesions[10,11] have also been discussed.

Although hyperostosis or arthritis of the anterior chest or axial region is often found in SAPHO syndrome,[2] involvement of the long bones is relatively rare. Few reports have compared the radiological features to the pathological findings. The purpose of this study was to demonstrate the radiological and histopathological features of long bone lesions in SAPHO syndrome and to correlate these with the clinical findings.

H. Orui (✉) · M. Takahara · A. Ishikawa · M. Takagi · T. Tsuchiya · T. Ogino
Department of Orthopaedic Surgery, Yamagata University School of Medicine, 2-2-2 Iida-nishi, Yamagata 990-9585, Japan
Tel. +81-23-628-5355; Fax +81-23-628-5357
e-mail: hoorui@med.id.yamagata-u.ac.jp

Materials and methods

The diagnosis of SAPHO syndrome was made using the criteria advocated by Benhamou et al. Sixteen patients, 4 male and 12 female, were diagnosed as having SAPHO syndrome in Departments of Orthopaedic Surgery, Yamagata University School of Medicine, between 1979 and 1999. Of these patients, six had long bone lesions, on which radiography, ^{99m}technetium bone scintigraphy, computed tomography (CT) scan, and magnetic resonance imaging (MRI) were performed. The present study includes these six cases and a case with long bone lesions diagnosed at Department of Orthopaedic Surgery, Date Red Cross Hospital. In six of the cases, bone biopsy and bone culture were performed.

Results

Clinical findings

Case 1. A 6-year-old boy presented with a 9-month history of left gonalgia and lumbago. Palmoplantar pustulosis and tonsillitis had been occasionally observed before onset of the gonalgia. The gonalgia decreased 2 months after the bone biopsy, and the radiographic hyperostotic appearance disappeared gradually during the 6-year follow-up period.

Case 2. A 63-year-old woman consulted our clinic with a 1-year history of left thigh pain. She also had a 5-year history of PPP with pain in the anterior chest and pubis. Her condition temporarily deteriorated for a few weeks after the bone biopsy. Her complaints continued after the biopsy, although nonsteroidal antiinflammatory drugs (NSAIDs) provided partial pain relief.

Case 3. A 47-year-old woman consulted a clinic with a 5-day history of bilateral thigh pain after mountain climing. Palmoplantar pustulosis had been occasionally observed before the onset. Blood culture revealed positivity for staphylococcus epidermidis on consultation. Needle biopsy was performed for the shaft of the right tibia 2 weeks after the onset. The thigh pain decreased after treatment with antibiotics.

Case 4. A 57-year-old woman consulted our clinic with a 3-month history of right thigh pain. She had suffered from hyperthyroidism, PPP, tonsillitis, and ossification of the posterior longitudinal ligament of the cervical spine for several years before admission. Histopathologically, her resected tonsils showed T-zone hyperplasia with focal follicular hyperplasia. Four years after the tonsillectomy, her thigh pain had decreased gradually and osteosclerosis was resolved radiologically.

Case 5. A 68-year-old woman had suffered pain in the insertion of the left calcaneal tendon, multiple arthralgia (bilateral knee, left ankle, right shoulder), and PPP for 13 years. She consulted our clinic because of left gonalgia, and was treated as for rheumatoid arthritis for more than 10 years. Her symptoms were partially relieved with NSAIDs.

Case 6. A 37-year-old man consulted our clinic with a 4-month history of pain in the left upper arm. He had suffered from pustulosis and hyperkeratosis in the bilateral palm for several years. Omalgia and arm pain diminished immediately after the bone biopsy procedure.

Case 7. A 67-year-old man consulted his family doctor with buttock pain, and cortical erosion and intramedullary mineralization of the left femur was detected by radiograpy. He consulted our clinic with suspected bone cancer. He has suffered palmar and plantar pustulosis and hyperkeratotic change for several years.

The patients included three males and four females ranging in age from 6 to 63 years, with a mean age of 47 years. Six of the patients presented with pain related to the involved long bones, while one presented with only buttock pain (case 7). Six of the seven patients had polyostotic involvement, and another had gonalgia only (case 1). One patient exhibited multiple arthralgia (case 5). The duration of symptoms before bone biopsy ranged from 0.5 to 12 months, with a mean duration of 6 months. None of the patients had experienced trauma or fever. All seven patients exhibited PPP, or palmar or plantar hyperkeratosis. One of the seven patients suffered from chronic tonsillitis (case 4).

The duration of follow-up ranged from 4 to 78 months, with a mean of 31 months. Pain decreased in four patients (cases 1, 3, 4, and 6), of whom one (case 4) showed a gradual pain decrease for 4 years after tonsillectomy. Pain in another patient decreased immediately after biopsy of the humerus without any radiological change (case 6). One of the three patients (case 1) improved radiologically during more than 60 months of follow-up. The remaining three patients showed no clinical change.

Laboratory data at examination showed increase in erythrocyte sedimentation rate (ESR) in four cases of seven. White blood cell number was increased only one case of seven. Mild increase in C reactive protein (CRP) was detected in five cases of seven. Rheumatoid factor was negative in four cases of four. Dysimmunoglobrinemia was revealed in two of two cases (cases 2, 5). CH50 was increased in three of three cases (cases 2, 5, 6). HLA-B27 was examined only in one case and showed negativity (case 6). A summary of the clinical and laboratory data is presented in Tables 1 and 2.

Radiographic findings

In the present study, the long bone lesions of the syndrome on plain films showed hyperostosis, osteolysis, and intramedullary mineralization. Two long bones of two patients showed hyperostosis or massive cortical thickening in the femoral shaft (cases 1, 2) (Fig. 1A). Hyperostosis of right femoral shaft in case 1 recovered to normal radiological appearance 5 years after the onset, whereas, in the lesion

Table 1. SAPHO syndrome involving long bones: clinical data

Case	Age at examination (years)/sex	Duration before examination (months)	Site of pain	Dermatosis	Past history	Follow-up duration (months)	Pharmacologic treatment	Clinical change of long bone	Radiologic change of long bone
1	6/F	11	Thigh (l)	PPP	Allergic dermatitis, tonsillitis	60	Antibiotics	Improved	Improved
2	63/F	12	Thigh (l)	PPP	Gastric ulcer	20	NSAID	No	No
3	47/F	0.5	Thigh (b)	PPP	No	6	Antibiotics	Improved	Improved
4	57/F	4	Thigh (r)	PPP	Grave's, OPLL, chronic tonsilitis, cholelithiasis	78	NSAID	Improved	No
5	55/F	12	Thigh (r), multiple arthralgia	PPP	No	4	NSAID	No	No
6	37/M	6	Arm (l)	PPP Tinea	No	5	NSAID	Improved	No
7	67/M	3	Buttock (l)	PPP	No	47	NO	No	No

SAPHO, Synovitis, acne, pustulosis, hyperostosis, osteitis; l, left; r, right; PPP, palmoplantar pustulosis; OPLL, ossification of posterior longitudinal ligament; NSAID, nonsteroidal antiinflammatory drug

Table 2. SAPHO syndrome involving long bones: laboratory data at examination

Case	WBC (/μl)	HB (g/dl)	TP (g/dl)	A/G	ESR (mm/h)	CRP (mg/dl)	RF (mg/dl)	Dysimmunoglobulinemia	Complement (CH50/ml)	HLA-B27
1	10700	13.5	8.2	NA	8	<0.2	NA	NA	NA	NA
2	6900	11.6	7.9	1.51	62	0.5	<10	IgA ↑	49 ↑	NA
3	7800	12.1	6.4	1.13	60	1.6	NA	NA	NA	NA
4	7900	12.9	7.9	1.08	22	0.6	–	NA	NA	NA
5	4800	8.7	8.0	0.9	70	1.4	<9	IgA ↑	58 ↑	NA
6	3570	16.6	7.6	2.12	2	0.6	<10	NA	53 ↑	–
7	4870	14.2	8.3	1.33	14	<0.1	NA	NA	NA	NA

HB, hemoglobin; TP, total protein; A/G, albumin globulin ratio; ESR, erythrocyte sedimentation rate; CRP, C-reactive protein; RF, rheumatoid factor; NA, not applicable

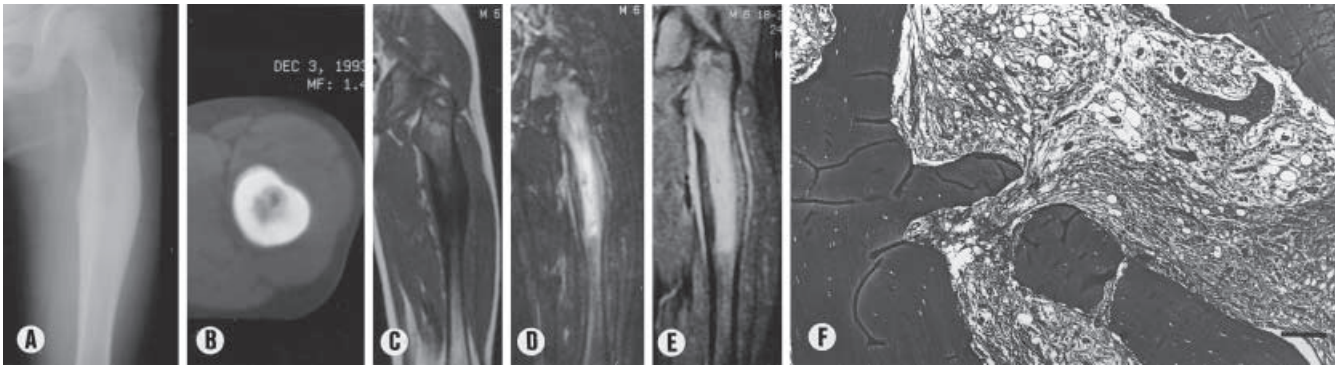

Fig. 1. Case 1. Plain radiography (**A**) and computed tomography (CT) scan (**B**) show hyperostosis of femoral shaft. On magnetic resonance imaging (MRI), the lesion shows low signal intensity on T_1-weighted image (WI) (**C**), high signal intensity on short tau inversion recovery (STIR) (**D**), and enhancement with gadolinium on T_1-WI (**E**). Biopsy specimen shows marrow fibrosis with inflammatory cell infiltration (hematoxylin-eosin). *Bar* 125 μm (**F**)

of case 2, no recovery was found 2 years after the biopsy. Six long bones of four patients showed osteolysis of the cortical bone in the femoral diaphysis (cases 3, 4), metaphysis (cases 5), or proximal tibia (case 7); these were frequently accompanied by cortical sclerosis (cases 3–5), presenting mixed lytic and sclerotic features (Figs. 2, 3). In case 3, cortical bone absorption was observed in bilateral femoral shafts 3 weeks after the onset (Fig. 2B). Even nonbiopsied lesions showed linear periosteal reaction 12 weeks after the onset (Fig. 2C) and changed to hyperostosis 6 months after the onset (Fig. 2D). The biopsied side showed a similar reparative process to the nonbiopsied side. In case 4, radiography showed mild thickening of the right femoral cortical bone with cortical surface irregularity (Fig. 3A). In case 5, an

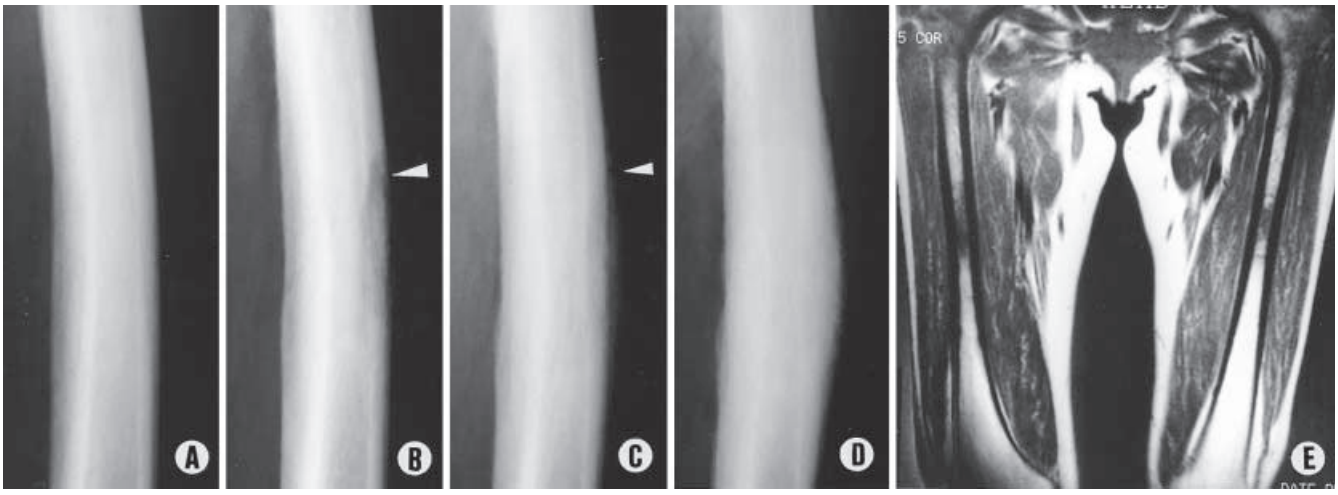

Fig. 2. Case 3. Plain radiography of the left femoral shaft (nonbiopsy side) shows no marked change at consultation (**A**), radiolucency (*arrowhead*) of the cortex bone 3 weeks after onset (**B**), linear periosteal reaction (*arrowhead*) 12 weeks after onset (**C**), and cortical thickening 6 months after onset (**D**). MRI demonstrates nonhomogenous low signal intensity of intramedullary lesions of bilateral femoral shaft on T_1-WI (**E**)

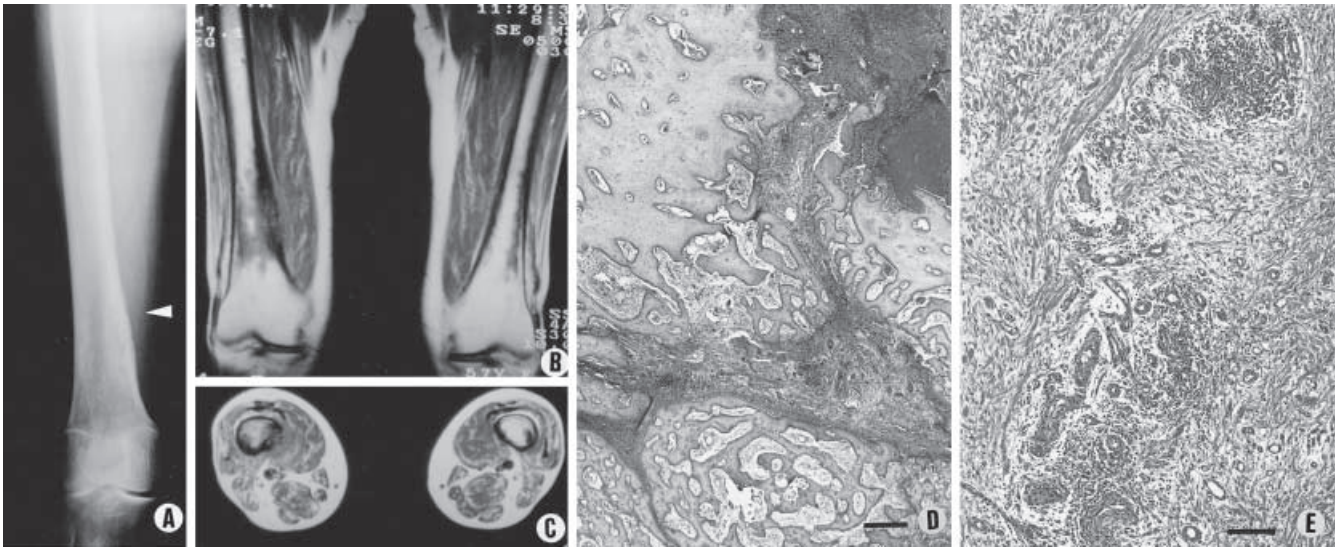

Fig. 3. Case 4. Plain radiography shows cortical thickening and irregularity of the femoral shaft (*arrowhead*) (**A**). MRI demonstrates low signal intensity of bilateral femoral shafts and cortical thickening of right femoral shaft on T_1-WI (**B,C**). Biopsy specimen shows mixture of bone necrosis and new bone formation with marrow fibrosis (hematoxylin-eosin; *bar* 250 μm) (**D**) and inflammatory cell aggregation (hematoxylin-eosin; *bar* 125 μm) (**E**)

insufficiency fracture was accompanied in the right femoral metaphysis, and a cyst with marginal sclerosis was observed in the left proximal tibia. On the other hand, diffuse bone atrophy with focal sclerosis was observed in the right proximal tibia in case 7. Two bones in two patients showed cortical thinning with intramedullary mineralization in the humeral metaphysis and diaphysis and femoral diaphysis (cases 6, 7), suggesting bone infarction (Fig. 4A, 5A).

On CT scan, cases showing hyperostosis described marked cortical thickening (cases 1, 2) (Fig. 1B). Cases showing bone absorption described cortical irregularity with mild cortical thickening (case 3–5). Cases with intramedullary mineralization revealed intramedullary mineralized shells in the neck and shaft (case 6) or a high-density mineralized mass (case 7).

Comparing the MR images with their radiological findings, hyperostosis was described as a homogenous low signal intensity intramedullary area on T_1-weighted image (T_1-WI) (cases 1, 2). The lesions were described as low signal intensity on T_2-WI and short tau inversion recovery (STIR) and were well enhanced by gadolinium on T_1-WI in case 1 (see Fig. 1), whereas they were described as low signal on T_2-WI and STIR and scarcely enhanced by gadolinium on T_1-WI in case 2. Osteolytic lesion showed low

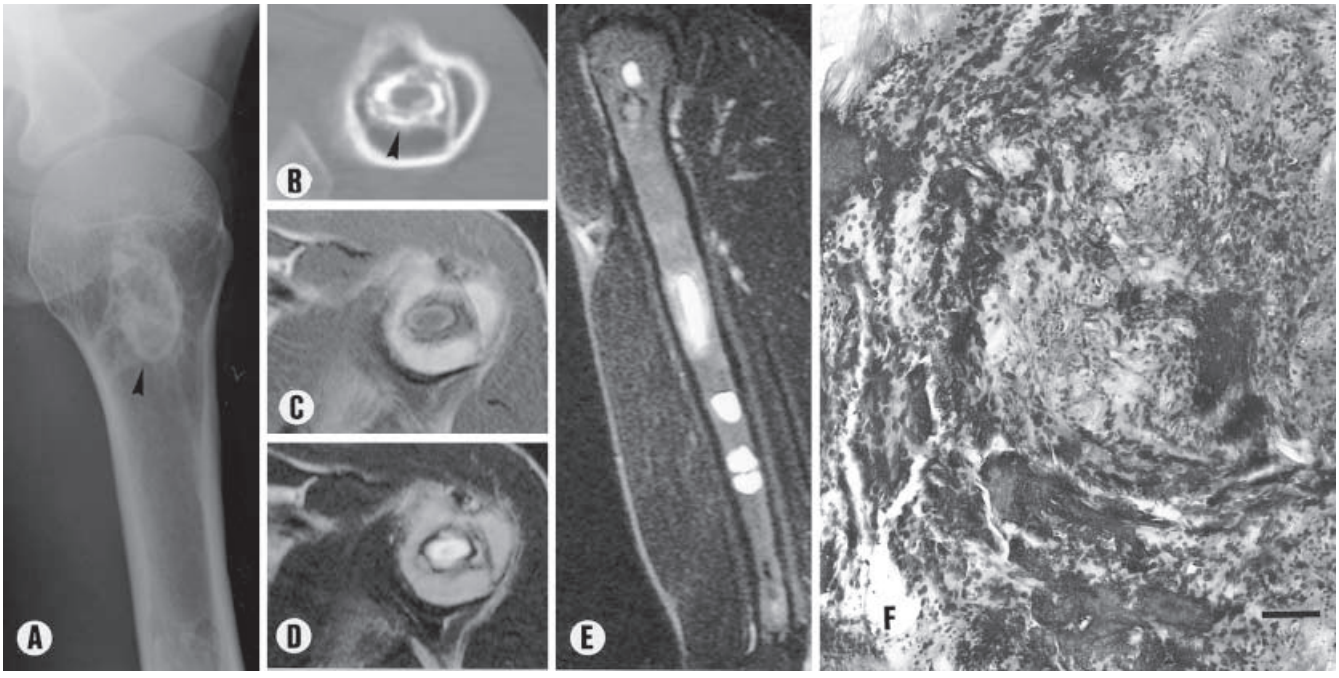

Fig. 4. Case 6. Plain radiography (**A**) and CT scan (**B**) show intramedullary sclerotic rim (*arrowheads*). MRI demonstrates cystic lesions in the intramedullary sclerosis on T_1-WI (**C**), STIR (**D**), and gadolinium-enhanced T_1-WI (**E**). Dystrophic calcification is demonstrated in the cystic lesions (hematoxylin-eosin; *bar* 125 μm) (**F**)

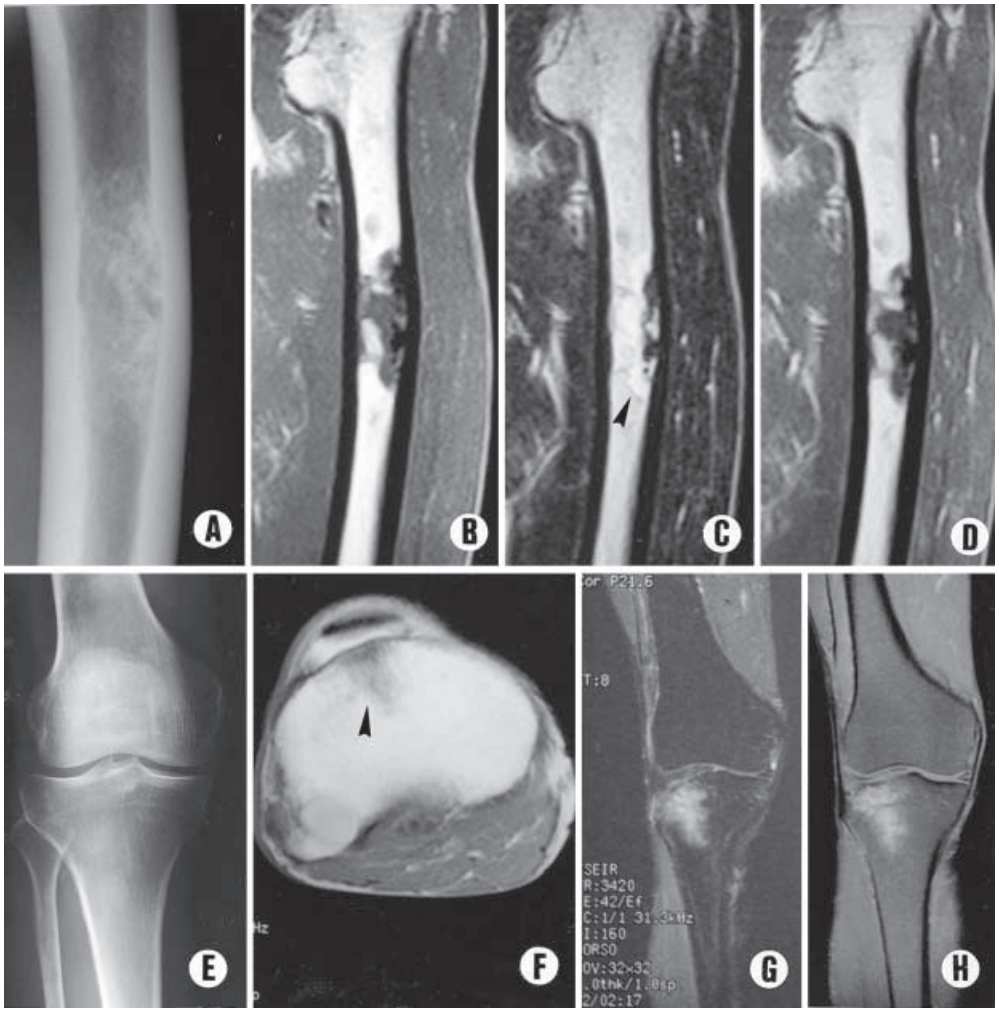

Fig. 5. Case 7. Plain radiography of the left femur shows intramedullary mineralization (**A**). MRI demonstrates cystic lesions in the intramedullary sclerosis on T_1-WI (**B**), T_2-WI (*arrowhead*) (**C**), and gadolinium-enhanced T_1-WI (**D**). Plain radiography of the right proximal tibia shows radiolucency with focal sclerosis (**E**). MRI demonstrated low signal intensity on T_1-WI (*arrowhead*) (**F**), high signal intensity on STIR (**G**), and gadolinium enhancement on T_1-WI fat suppression image (**H**)

signal intensity on T_1-WI, high signal intensity on T_2-WI, and enhancement by gadolinium on T_1-WI (case 3, proximal tibia in case 7). A mixed lytic and sclerotic lesion was described as a nonhomogenous low signal intensity-thick cortical and intramedullary area on T_1-WI, high signal intensity on T_2-WI, and enhanced by gadolinium on fat suppressed T_1-WI (cases 4, 5) (Fig. 4). In cases 6 and 7, intramedullary mineralization was described as a low signal intramedullary area on T_1- and T_2-WI. These lesions were accompanied by areas showing low signal intensity on T_1-WI, high signal intensity on T_2-WI and STIR, and no enhancement with gadolinium on T_1-WI. These findings indicated cystic lesions. In these cases, intramedullary mineralization on plain film and CT was delineated as low signal intensity masses on T_1- and T_2-WI.

The long bone lesions in the cases, except for the humeral lesion in case 6 and femoral lesion in case 7, showed abnormally high accumulation on bone scintigraphy.

Histopathological findings and bone culture

All cases that were biopsied showed bone marrow fibrosis and inflammatory cell infiltration composed of lymphocytes compatible with chronic osteomyelitis (cases 1–4, 6, 7).

Hyperostotic lesions (cases 1, 2) demonstrated histologically bone marrow fibrosis, new bone formation, and bone necrosis. Of these cases, lesions showing high signal intensity on T_2-WI with gadolinium enhancement on T_1-WI (case 1) on MRI demonstrated loose fibrosis with plasma-cell rich inflammation. On the other hand, lesions showing low signal intensity on T_2-WI without gadolinium enhancement on T_1-WI demonstrated marked bone necrosis with inflammatory necrotic debris with scarcely observed inflammatory cell infiltration.

Osteolytic lesions demonstrated bone marrow fibrosis with plasma cell-rich (case 3) or granulocyte and lymphocyte infiltration (proximal tibia of case 7). In contrast, mixed lytic and sclerotic lesion (case 4) demonstrated creeping substitution or mosaic pattern observed in Paget's disease with focal inflammatory cell infiltration corresponding to the nonhomogenous enhancement on MRI.

Lesions showing bone cyst or mineralization radiologically (case 6, femoral shaft in case 7) correspond histologically to necrotic bone, fibrosis, dystrophic calcification, and chronic inflammatory cell infiltration, suggesting bone infarction. In each case, bone culture was negative for aerobic, anaerobic, and acid-fast bacteria as well as fungal organisms at the time of biopsy.

Discussion

The diagnosis of SAPHO syndrome is established using the criteria formulated by Benhamou et al.[12] According to the criteria, this syndrome can be diagnosed by (1) hyperostosis or chronic recurrent multifocal osteomyelitis (CRMO) or (2) other osteo-articular manifestations in association with dermatologic conditions such as acne conglobata, acne fulminans, or PPP. In this study, cases 1 and 2 could be diagnosed by the hyperostosis alone, although PPP was present in both cases. Cases 3 to 6 were diagnosed by the osteo-articular manifestations associated with PPP.

In previous reports, the long bone lesions of SAPHO syndrome occurred in approximately 30% of the patients, and osteosclerosis, osteolysis and periosteal new bone formation suggesting infectious or tumorous conditions were demonstrated.[13,14] In this study, the long bone lesions of SAPHO syndrome can show radiologically not only hyperostosis but also osteolysis or bone infarction-like features.

Hyperostosis involved the shaft of long bones (cases 1, 2), and rarely involved an epiphyseal lesion. Radiography and CT demonstrated thick cortical bone. On MRI, the lesions showed low signal intensity on T_1- and T_2-WI, and were enhanced with gadolinium on T_1-WI depending on inflammatory or ossification activity. Histological findings of this lesion included massive bone necrosis or periosteal new bone formation with chronic inflammatory cell infiltration.

Osteolysis with or without sclerosis can be observed any site of the long bones. For instance, an epiphyseal lesion was found in cases 5 and 7, metaphyseal lesions in case 5, and diaphyseal lesions in cases 3 and 4. Osteolysis was often accompanied by sclerosis. Radiography and CT demonstrated osteolysis with or without mild cortical sclerosis. On MRI, osteolytic lesion demonstrated low signal intensity on T_1-WI, high signal intensity on T_2-WI, and gadolinium enhancement on T_1-WI, even if the lesion was accompanied by sclerosis (cases 4, 5). Histologically, these lesions showed granulation, necrotic bone, new bone formation, bone marrow fibrosis, and acute or chronic inflammatory cell infiltration.

Intramedullary calcification and sclerosis suggested bone infarction radiologically. Pathologically, marrow fibrosis, calcification, and cystic change were compatible with bone infarction. On MRI, fibrosis with calcification showed low signal intensity on T_1- and T_2-WI, and demonstrated no gadolinium enhancement on fat suppression T_1-WI.

These radiological appearances may reflect the stage and activity of inflammation. In case 3, although the femur showed no change radiologically on consulting the hospital, osteolysis appeared 2 weeks after consultation, followed by cortical thickening 6 months after consultation. In case 1, the hyperostotic change of the femur recovered to normal appearance during several years. On the other hand, hyperostosis can remain (case 2) if recovery is not sufficient. Furthermore, bone remodeling may not occur sufficiently when the lesion is restricted to the intramedullary area (cases 6, 7). These findings suggest the hypothesis that osteolysis and hyperostosis reflect not only their bone-forming activity but also their clinical stage and the place of the inflammation.

Vande Berg classified MRI of the bone marrow lesions on T_1-WI into four categories: marrow depletion, marrow infiltration, marrow replacement, and signal void, depending on the fat–nonfat marrow balance.[15] In the present study, hyperostotic lesions corresponded to marrow replacement or marrow signal void. Osteolysis was demon-

Table 3. SAPHO syndrome involving long bones: radiographic findings

Case	Sites involved	Plain film	CT	MRI	High accumulation on bone scintigraphy
1	FD (l)	Hyperostosis Lamellar periosteal reaction	Marked cortical thickening	Cortical and intramedullary low signal intensity on T_1- and T_2-WI, with Gd	FD (l)
2	FD (l)	Hyperostosis	Marked cortical thickening	Cortical and intramedullary low signal intensity on T_1- and high on T_2-WI, without Gd	FD (l), P, SC
3	FD (b)	Osteolysis, →periosteal reaction	→Mild cortical thickening	Inhomogenous, intramedullary, low signal on T_1-WI and high signal on T_2-WI	FD (b)
4	FD (b)	Osteolysis, sclerosis	Mild cortical thickening	Nonhomogenous, intramedullary, low signal on T_1-WI and high signal on T_2-WI	FD (r), SC
5	FM (r)	Osteolysis, sclerosis, insufficient fracture	Mild cortical thickening	Nonhomogenous, intramedullary, low signal on T_1-WI and high signal on T_2-WI	FD (r), T (l), SC
	TE (l)	Osteolysis Intramedullary ossification	NA	NA	
6	HD (l)	Intramedullary mineralization	Intramedullary mineralization	Intramedullary intermediate signal with low marginal area on T_1-WI, high signal with low marginal area on T_2-WI, without Gd	IS, SC
7	FD (l)	Intramedullary calcification	Intramedullary calcification	Intramedullary intermediate signal on T_1-WI, low signal and high signal areas on T_2-WI, without Gd	TE (r), IS, SC
	TE (r)	Osteolysis, focal sclerosis	NA	Low signal on T_1-WI, high signal on T_2-WI, with Gd	

F, femur; T, tibia; H, humerus; D, diaphysis; M, metaphysis; E, epiphysis; SC, sternclavicular; IS, iliosacral; WI, weighted image; Gd, gadolinium enhancement

Table 4. SAPHO syndrome involving long bones: histopathological findings

Case	Site biopsied	Histological findings			
		Bone necrosis	New bone formation	Bone marrow fibrosis	Inflammatory cell infiltration
1	FD (l)	Massive	Creeping substitution	Loose	Plasma cell rich
2	FD (l)	Massive	Creeping substitution	Dense fibrosis, necrotic debris	Scarce
3	FD (r)	Scarce	No	Loose	Plasma cell rich
4	FD (r)	Massive	Creeping substitution	Dense fibrosis, necrotic debris	Focal lymphocyte aggregation
6	HD (l)	Massive	Scarce	Dense fibrosis, necrotic debris, calcification	Scarce
7	FD (l)	Massive	Scarce	Dense fibrosis, necrotic debris, calcification	Scarce
7	TE (r)	Scarce	Scarce	Dense fibrosis, necrotic debris	Acute and chronic inflammatory cell infiltration

F, femur; T, tibia; H, humerus; D, diaphysis; E, epiphysis

strated as marrow infiltration or marrow replacement. STIR revealed well the cystic lesion and osteolytic lesions. Furthermore, gadolinium enhancement delineated osteolysis and new bone formation. MRI can represent the histopathological findings of long bone lesions of SAPHO syndrome.

The differential diagnosis of long bone lesions in SAPHO syndrome is problematic[16,17] because the radiological features are often atypical compared to the anterior chest lesions. Furthermore, the laboratory data show no specific findings. In this study, cases 3 to 7 did not show marked hyperostosis, and case 1 did not have costoclavicular or spondylotic lesions. In the present study, cases showing hyperostosis had to be distinguished from osteoid osteoma, osteoblastoma, osteoma, and fibrous dysplasia. Cases showing osteolysis had to be distinguished from suppurative osteomyelitis, Paget's disease, fibrous dysplasia, and malignant bone tumor such as Ewing sarcoma and osteosarcoma.[16] If the lesion shows intramedullary mineralization, chondrosarcoma has to be distinguished.

In conclusion, the present study demonstrated the radiological features of long bone lesions of SAPHO syndrome, corresponding to their pathological findings. Furthermore, the lesions do not always show hyperostosis but also show osteolysis or bone infarction-like lesions.

Acknowledgments We thank Dr. Mitsugu Yoshida, Department of Orthopaedic Surgery, Date Red Cross Hospital, for providing clinical data of a case.

References

1. Sasaki T. A case with osteomyelitis of the bilateral clavicles association with pustulosis palmaris et plantaris. Rinsho Seikeigeka 1967;2:333–7.
2. Chamot AM, Benhamou CL, Beraneck L, Kahn MF, Kaplan G, Prost A. S.A.P.H.O.: syndrome acne pustulose hyperostose osteite. Rev Rhum 1987;54:187–96.
3. Köhler H, Uehlinger E, Kutzner J, West T. Sternocosto-klaviculare Hyperostose: ein bisher nicht beschreibenes Krankheitsbild. Dtsch Med Wochenschr 100;1519–23.
4. Collert S, Isacson J. Chronic sclerosing osteomyelitis. Clin Orthop 1980;164:136–40.
5. Giedion A, Holthusen W, Masel LF. Subacute and chronic "symmetrical" osteomyelitis. Ann Radiol Paris 1972;15:329–42.
6. Bjorksten B, Boquist L. Histopathological aspects of chronic recurrent multifocal osteomyelitis. J Bone Joint Surg 1980;62B:376–81.
7. Sonozaki H, Mitsui H, Miyanaga Y. Clinical features of 53 cases with pustulotic arthroosteitis. Ann Rheum Dis 1981;40:547–53.
8. Maugar Y, Berthelot J-M, Ducloux J, Prost A. SAPHO syndrome: a followup study of 19 cases with special emphasis on enthesis involvement. J Rheumatol 1995;22:2135–41.
9. Winchester R. Psoriatic arthritis and spectrum of syndromes related to the SAPHO (synovitis, acne, pustulosis, hyperostosis, and osteitis) syndrome. Curr Opin Rheumatol 1999;11:251–6.
10. Sakai T, Kawaguchi M, Ishizawa S, Kaji T, Kitazawa K, Koizumi F. Histological features of palatine tonsils in pustulosis palmasis et plantaris: a morphometric study. Pathol Int 1994;44:186–93.
11. Girshick HJ, Huppertz H, Harmsen D, Krauspe R, Müller-Hermlink HK, Papadopoulos T. Chronic recurrent multifocal osteomyelitis in children: diagnostic vaqlue of histopathology and microbial testing. Hum Pathol 1999;30:59–65.
12. Benhamou CL, Chamot AM, Kahn MF. Synovitis-acne-pustulosis-hyperostosis-osteomyelitis syndrome (SAPHO): a new syndrome among the spondyloarthropathies? [Editorial]. Clin Exp Rheumatol 1988;6:109–12.
13. Cotton A, Flipo R-N, Mentre A, Delaporte E, Duquesnoy B, Chastanet P. SAPHO syndrome. Radiographics 1995;15:1147–54.
14. Kasperczyk A, Freyschmidt J. Pustulotic arthroosteitis: spectrum of bone lesions with palmoplantar pustulosis. Radiology 1994; 191:207–11.
15. Vande Berg BC, Malghem J, Lecouvet FE, Maldague B. Classification and detection of bone marrow lesion with magnetic resonance imaging. Skeletal Radiol 1998;27:529–45.
16. Reith JD, Bauer TW, Schil JP. Osseous manifestations of SAPHO (synovitis, acne, pustulosis, hyperostosis, osteitis) syndrome. Am J Surg Pathol 1996;20:1368–77.
17. Eyrich GKH, Harder C, Sailer HF, Langenegger T, Bruder E, Michek BA. Primary chronic osteomyelitis associated with synovitis, acne, pustulosis, hyperostosis and osteitis (SAPHO syndrome). J Oral Pathol Med 1999;28:456–64.